nature geoscience

REVIEW ARTICLE

PUBLISHED ONLINE: 23 OCTOBER 2011 | DOI: 10.1038/NGEO1296

Signatures of the Antarctic ozone hole in Southern Hemisphere surface climate change

David W. J. Thompson[1]*, Susan Solomon[2,3], Paul J. Kushner[4], Matthew H. England[5], Kevin M. Grise[1] and David J. Karoly[6]

Anthropogenic emissions of carbon dioxide and other greenhouse gases have driven and will continue to drive widespread climate change at the Earth's surface. But surface climate change is not limited to the effects of increasing atmospheric greenhouse gas concentrations. Anthropogenic emissions of ozone-depleting gases also lead to marked changes in surface climate, through the radiative and dynamical effects of the Antarctic ozone hole. The influence of the Antarctic ozone hole on surface climate is most pronounced during the austral summer season and strongly resembles the most prominent pattern of large-scale Southern Hemisphere climate variability, the Southern Annular Mode. The influence of the ozone hole on the Southern Annular Mode has led to a range of significant summertime surface climate changes not only over Antarctica and the Southern Ocean, but also over New Zealand, Patagonia and southern regions of Australia. Surface climate change as far equatorward as the subtropical Southern Hemisphere may have also been affected by the ozone hole. Over the next few decades, recovery of the ozone hole and increases in greenhouse gases are expected to have significant but opposing effects on the Southern Annular Mode and its attendant climate impacts during summer.

Roughly 90% of atmospheric ozone is found in the lower stratosphere in the ozone layer. Since about the 1970s, anthropogenic emissions of ozone-depleting gases have led to depletion of ~3–4% of the total overhead ozone averaged over the globe[1]. The strongest depletion is found over Antarctica during spring, when photochemical processes combine with a unique set of meteorological conditions to greatly increase the effectiveness of ozone-depleting gases, and more than half of the total overhead ozone is destroyed. Characteristics of the resulting Antarctic ozone hole are reviewed in refs 1 and 2, and the identification and attribution of the phenomenon was recently celebrated in a special edition of *Nature* (http://www.nature.com/nature/focus/ozonehole/).

The Antarctic ozone hole is evident in ozone observations taken every spring since about the early 1980s[1]. Its annual onset coincides with the return of sunlight to the cold polar stratosphere during September/October, and its decay with the collapse of the stratospheric vortex during November/December[1,2]. The most obvious surface impact is an increase in ultraviolet radiation reaching the surface[1]. Over the past decade, however, it has become clear that the ozone hole is also associated with widespread changes in the Southern Hemisphere tropospheric circulation and surface climate. Our purpose here is to review the evidence that suggests that the Antarctic ozone hole has had a demonstrable effect on the surface climate of the Southern Hemisphere.

The ozone hole and Southern Hemisphere circulation

Ozone absorbs incoming solar radiation. Hence the depletion of ozone over Antarctica leads to cooling of the polar stratosphere[2,3]. Basic atmospheric dynamics dictate that the resulting changes in the north–south temperature gradient must be accompanied by changes in the vertical shear of the wind. As a result, the ozone hole leads to an acceleration of the stratospheric polar vortex (a region of strong eastward circumpolar flow) during October–December[4].

The differences in the Southern Hemisphere polar stratosphere between the pre-ozone-hole and ozone-hole eras are highlighted in Fig. 1. The ozone hole is associated with monthly mean decreases in lower stratospheric ozone that exceed 80% during October–November and exceed 20% throughout the austral autumn and winter seasons (Fig. 1a). The corresponding changes in polar stratospheric geopotential height (Z) are indicative of a strengthening of the eastward circumpolar flow that also peaks during the late austral spring season and persists through January [4,5] (Fig. 1b; polar Z provides a close estimate of the north–south gradient in Z across ~55–65° S, and thus the strength of the circumpolar flow).

The eastward acceleration of the lower stratospheric flow due to ozone depletion is interesting in its own right. What makes the acceleration particularly relevant for climate change is that it extends to the Earth's surface during the summer months (Fig. 1b). Deep vertical coupling between the circumpolar tropospheric and stratospheric flow is observed on monthly and daily timescales in both the Northern and Southern Hemispheres[6–9]. The changes in the tropospheric flow indicated in Fig. 1b suggest that such coupling is also characteristic of the ozone hole.

The summertime falls in Z in the polar troposphere (Fig. 1b; Fig. 2a) are accompanied by rises at middle latitudes (Fig. 2a). The pattern of Z changes in Fig. 2a strongly resembles the high-index polarity of the leading mode of climate variability in the Southern Hemisphere troposphere, known as the Southern Annular Mode (SAM). In the troposphere, the SAM is characterized by nearly zonally symmetric, north–south variability in the latitude of the midlatitude jet and its associated wave fluxes of heat and momentum[6,10–12]. The high-index polarity of the SAM is marked by poleward displacements of the jet and thus by strengthening of the prevailing atmospheric eastward

[1]Department of Atmospheric Science, Colorado State University, Fort Collins, Colorado 80523, USA, [2]NOAA Chemical Sciences Division, University of Colorado, Boulder, Colorado 80309-0311, USA, [3]Department of Atmospheric and Oceanic Sciences, University of Colorado, Boulder, Colorado 80309-0311, USA, [4]Department of Physics, University of Toronto, 60 St George Street, Toronto, Ontario M5S 1A7, Canada, [5]Climate Change Research Centre, Faculty of Science, University of New South Wales, Sydney, New South Wales 2052, Australia, [6]School of Earth Sciences, University of Melbourne, Melbourne, Victoria 3010, Australia. *e-mail: davet@atmos.colostate.edu

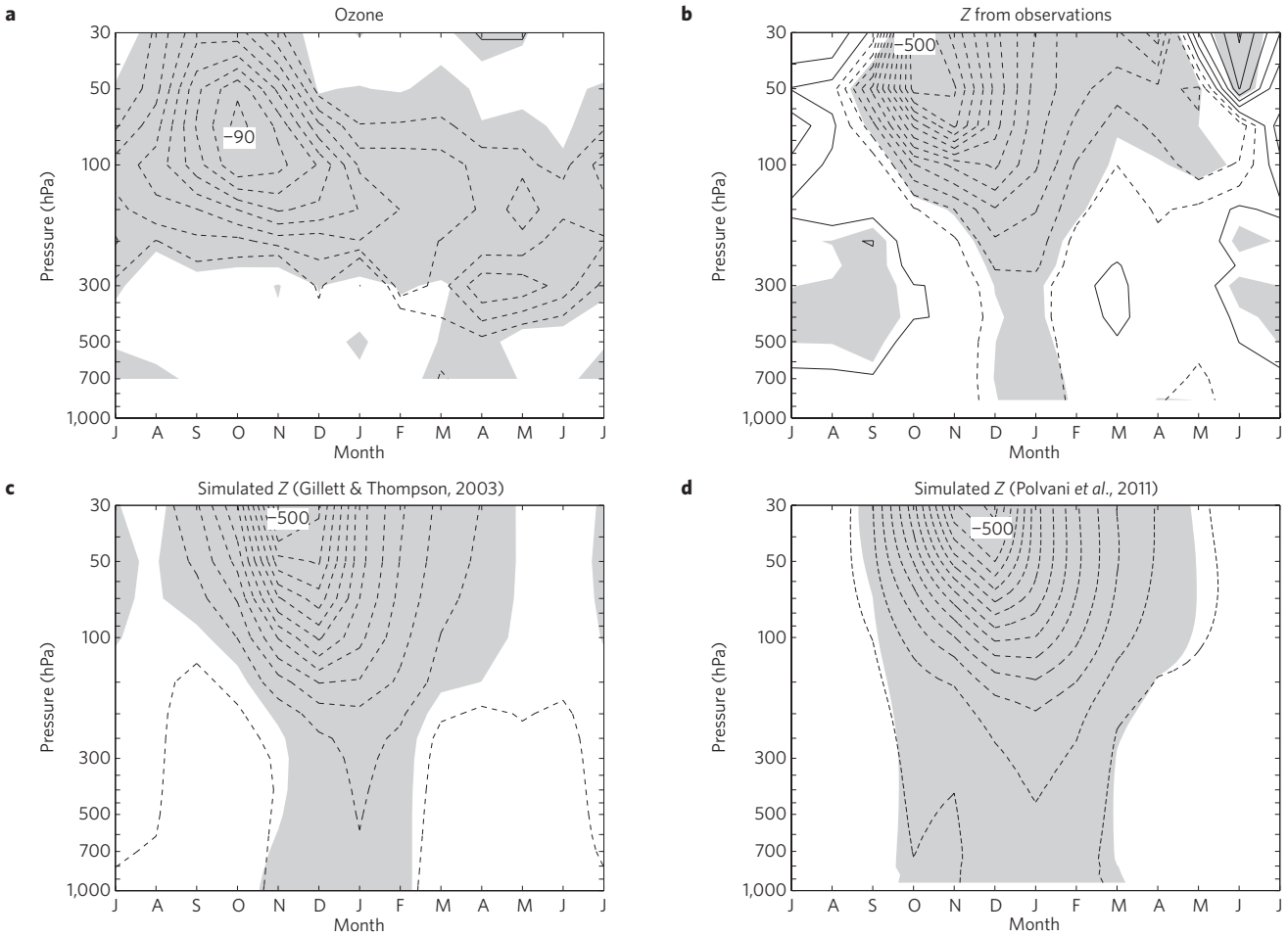

Figure 1 | Signature of the ozone hole in observed and simulated changes in the Southern Hemisphere polar circulation. a,**b**, Observed composite differences between the pre-ozone-hole and ozone-hole eras in (**a**) polar ozone from Syowa station (69° S, 40° E; similar results are obtained for other stations within the region of the ozone hole) and (**b**) polar-mean *Z* from radiosonde data. **c**,**d**, Simulated differences in polar *Z* between the pre-ozone-hole and ozone-hole eras from the experiments in refs 30 and 33. Contour intervals are (**a**) 10% depletion for values of 20% and greater and (**b**–**d**) 40 m (−60, −20, 20...). Positive contours are solid, negative contours are dashed. Shading indicates trends significant at the 95% level based on a one-tailed test of the *t*-statistic. See Methods for details.

flow near ~60° S; weakening of the prevailing atmospheric eastward flow near ~40° S; and reduced *Z* over the polar cap that extends from the surface to the stratosphere. The SAM owes its existence to internal tropospheric dynamics and vacillates between its high- and low-index polarities on timescales as short as weeks[11,13,14]. The observational evidence reviewed in Figs 1 and 2a suggests that the Antarctic ozone hole has perturbed the Southern Hemisphere circulation in a manner consistent with a trend in the SAM towards its high-index polarity.

Attribution of the observed trend in the SAM

The observed summertime trend towards the high-index polarity of the SAM between the pre-ozone-hole and ozone-hole eras has been shown to be statistically significant[15–17] and distinct from estimates of natural variability[15]. As discussed later in this Review, qualitatively similar trends towards the high-index polarity of the SAM are found in climate models forced by increasing greenhouse gases. Such simulations suggest that the influence of increasing greenhouse gases on the SAM will be appreciable over the twenty-first century but that it was modest over the past few decades. The available model evidence suggests that the recent trend in the SAM is due primarily to the development of the Antarctic ozone hole.

Supporting model evidence includes experiments run on: (1) idealized atmospheric general circulation models forced with imposed cooling in the polar stratosphere[18–20]; (2) global climate models for the IPCC Fourth Assessment Report (the third Coupled Model Inter-comparison Project, CMIP3), in which greenhouse gases increase and the ozone depletion is prescribed based on observations[15,21–25]; (3) coupled chemistry–climate models (for example as for the Coupled Chemistry Climate Model Validation Project, CCMVal1 and 2), in which the ozone depletion is calculated based on simulated chemical and dynamical processes[24,26–28]; (4) climate models forced solely with the observed changes in stratospheric ozone[29–34].

Results derived from all four types of experiments point to the robustness of the linkages between the Antarctic ozone hole and the SAM. But there are caveats. The experiments run on idealized climate models are valuable because they are readily reproducible and are not dependent on specific physical parameterizations. But the rudimentary representation of climate processes and idealized thermal forcings used in such experiments limit comparisons with observations. The analyses of the CMIP3 and CCMVal output make valuable use of existing climate simulations but also include forcings other than stratospheric ozone depletion. Furthermore, the ozone forcing used in such simulations varies from model to model: the CMIP3 experiments are forced by prescribed ozone, but the prescribed ozone is not standard across all experiments; ozone is

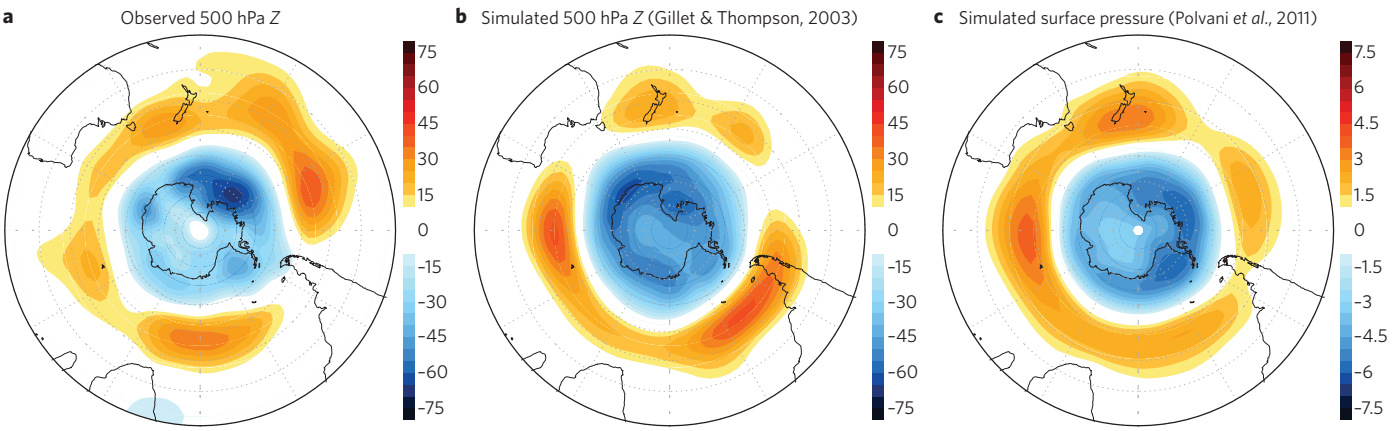

Figure 2 | Signature of the ozone hole in observed and simulated changes in the austral summertime circulation. a, Observed composite differences between the pre-ozone-hole and ozone-hole eras in mean December–February (DJF) 500-hPa *Z* from the NCEP-NCAR Reanalysis. **b**, Simulated differences in 500-hPa *Z* between the pre-ozone-hole and ozone-hole eras from the experiments in ref. 30. **c**, As in **b**, but for surface pressure from the experiments in ref. 33. The contour interval is 5 m in **a** and **b**, and 0.5 hPa in **c**. Values under 10 m (**a** and **b**) and 1 hPa (**c**) are not contoured.

predicted by the CCMVal models, and is thus necessarily different from experiment to experiment.

Arguably the most compelling model support for a causal link between the ozone hole and surface climate is derived from experiments in which only concentrations of (1) stratospheric ozone or (2) ozone-depleting substances are changed between integrations. Figures 1c, 1d, 2b, 2c, and 3 review the results from three such experiments: refs 30 and 33 in Figs 1 and 2, and ref. 28 in Fig. 3. The runs in refs 30 and 33 are 'time-slice' experiments: one 'slice' is forced with the seasonally varying distribution of stratospheric ozone before the development of the ozone hole; the other with the seasonally varying distribution of stratospheric ozone after the development of the ozone hole. The critical element in both experiments is that the only variable that is changed between slices is the distribution of ozone. The runs in ref. 28 are 'transient' simulations in which a coupled chemistry–climate model is forced by time-varying concentrations of greenhouse gases and/or ozone-depleting substances. Note that the time-slice experiments in refs 30 and 33 are forced by the observed changes in ozone whereas the transient experiments in ref. 28 are forced by changes in ozone-depleting substances (that is, the resulting changes in ozone are calculated by the model).

The time-slice experiments (refs 30 and 33) were forced with comparable changes in ozone, but were run on models with very different stratospheric resolution. One experiment (ref. 30) was run on a 'high top' model with extensive vertical resolution at stratospheric levels; the other (ref. 33) was run on a model with relatively poor stratospheric resolution (the model is typical of those used in the IPCC Fourth Assessment Report). Nevertheless, both experiments yield remarkably similar results (Fig. 1c and d; Fig. 2b and c). Both reveal pronounced changes in the stratospheric vortex during spring consistent with *in situ* forcing by the ozone hole. More importantly, both reveal substantial changes in the tropospheric circulation during the Southern Hemisphere summer consistent with the high-index polarity of the SAM (Fig. 2b and c). The most obvious difference between the simulated and observed changes lies in the timescale of the tropospheric response: the simulated responses extend from November to February whereas the observed responses are limited to December–January (Fig. 1).

The transient ozone-depletion experiments described in ref. 28 are driven in a very different manner from the time-slice experiments reviewed above. But again, the results confirm the importance of ozone depletion in driving past trends in the SAM towards its high-index polarity (Fig. 3a). Note that greenhouse forcing is important by the middle part of the twenty-first century, but not in the twentieth century (Fig. 3b). The changes in the SAM in response to future levels of ozone-depleting substances and greenhouse gases will be discussed later in this Review.

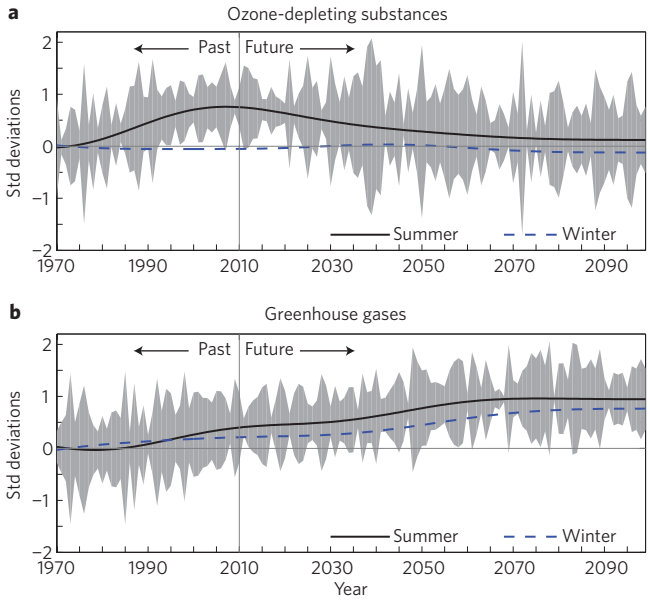

Figure 3 | Time series of the southern annular mode from transient experiments forced with time-varying ozone-depleting substances and greenhouse gases. Results are from experiments published in ref. 28. **a**, Forcing with ozone-depleting substances; **b**, forcing with greenhouse gases. The SAM index is defined as the leading principal component time series of 850-hPa *Z* anomalies 20–90° S: positive values of the index correspond to anomalously low *Z* over the polar cap, and vice versa. Lines denote the 50-year low-pass ensemble mean response for summer (DJF; solid black) and winter (JJA; dashed blue). Grey shading denotes ± one standard deviation of the three ensemble members about the ensemble mean (see Methods for details). The long-term means of the time series are arbitrary and are set to zero for the period 1970–1975. Past forcings are based on observational estimates; future forcings are based on predictions reviewed in ref. 28.

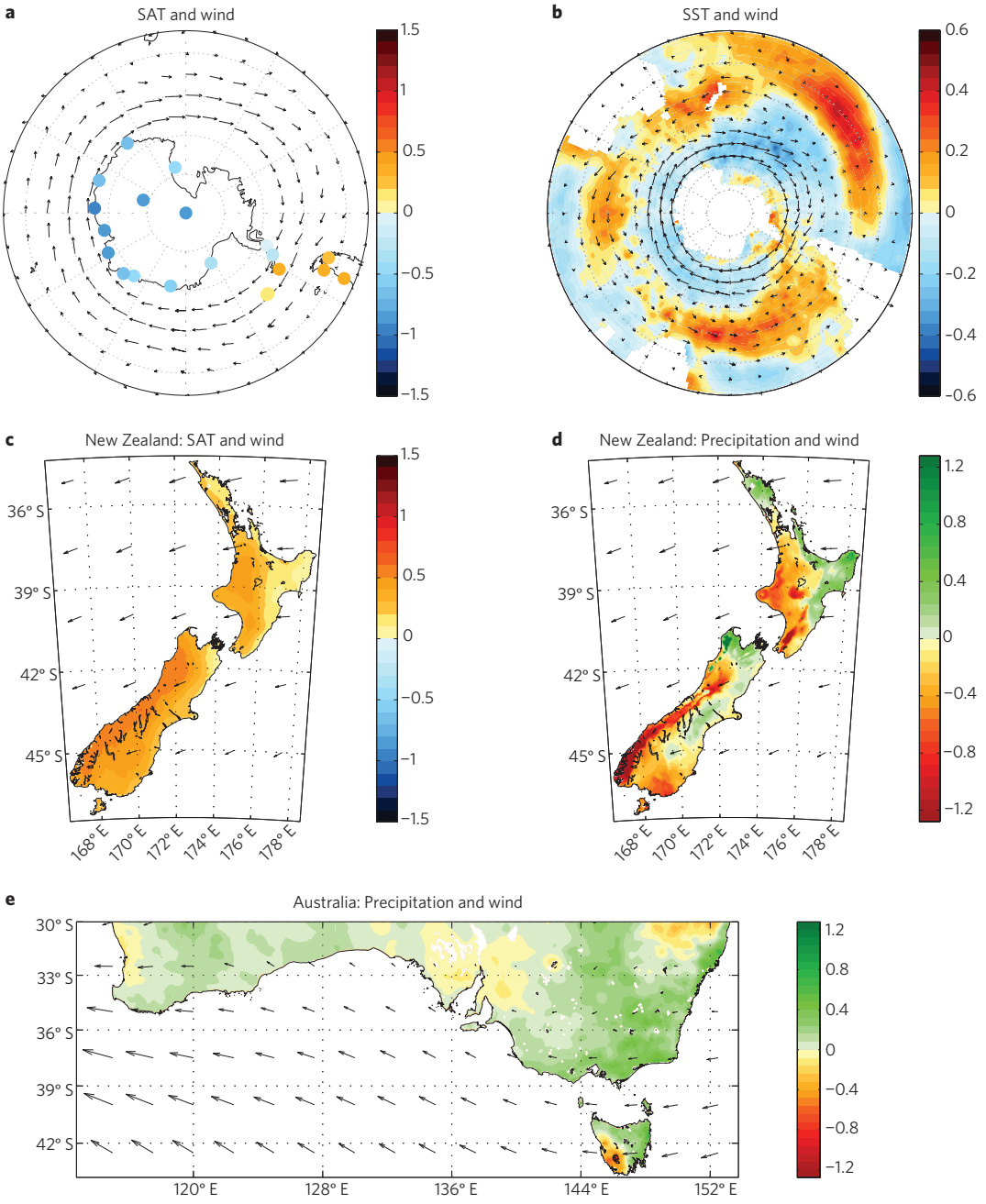

Figure 4 | Signature of the SAM in austral summertime climate variability. Results show regressions on the SAM index using DJF monthly mean data. **a**,**c**, Surface air temperatures (SAT; shading) and 925-hPa winds (vectors). **b**, Sea surface temperatures (SST; shading) and 925-hPa winds (vectors). **d**, **e**, Precipitation (shading) and 925-hPa winds (vectors). Shading interval is (**a** and **c**) 0.1 K; (**b**) 0.04 K; and (**d** and **e**) 0.08 mm day^{-1}. Data sources and analyses details are given in Methods.

How ozone depletion is linked to the SAM

The observed and modelled linkages between the ozone hole and tropospheric circulation anomalies resembling the SAM are robust. But the underlying mechanisms remain unclear. The principal problem is the following. We understand how the Antarctic ozone hole cools the polar stratosphere (mainly through reduced absorption of shortwave radiation). We understand why the polar cooling should lead to a strengthening of the Southern Hemisphere stratospheric polar vortex during spring (through geostrophic balance). But we do not fully understand the mechanisms whereby changes in the stratospheric polar vortex are coupled to variability in the tropospheric flow in the form of the SAM.

As noted earlier, the SAM owes its existence to internal tropospheric dynamics. Variability in the SAM is driven by changes in the fluxes of heat and momentum by synoptic-scale (1,000-km-scale) atmospheric waves[10–14]. In the case of the high-index polarity of the SAM, the changes in the wind field are driven by anomalous poleward wave fluxes of heat in the lower troposphere near 60° S and anomalous poleward wave fluxes of momentum at the tropopause. The link between the ozone hole and the SAM is thought to hinge critically on the effects of ozone depletion on these wave fluxes of heat and momentum.

One line of reasoning holds that stratospheric ozone depletion influences the SAM by means of its effect on the wave fluxes

of heat in the lower troposphere. Here the dynamics are based on the premises that: (1) the synoptic wave fluxes of heat in the lower troposphere are largely diffusive, that is, they are down-gradient and peak in regions of large temperature gradients and synoptic wave amplitudes[35]; and (2) the ozone hole perturbs the near-surface temperature gradient (and thus the diffusive wave fluxes of heat) both radiatively and dynamically.

The radiative forcing of the near-surface temperature gradient is straightforward. Stratospheric ozone depletion is accompanied by a reduction in downwelling longwave radiation through the polar tropopause, and thus cooling in the polar troposphere and an increase in the north–south temperature gradient near 60° S (ref. 36).

The dynamical forcing of the surface temperature gradient is more complicated. In this case, the strengthening of the Southern Hemisphere polar vortex changes the background conditions for planetary (greater than 6,000-km-scale) wave propagation, and thus the amplitude and location of the planetary wave breaking at stratospheric levels. The changes in stratospheric planetary wave breaking drive changes in atmospheric vertical motion that extend to the surface of the Earth (via downward control)[37–39]. In turn, the changes in vertical motion adjust the horizontal gradients in temperature through adiabatic expansion and compression.

A second line of reasoning holds that stratospheric ozone depletion influences the SAM through its effect on the strength of the lower stratospheric flow and the wave fluxes of momentum at the tropopause level. Numerical experiments suggest that changes in the lower stratospheric flow influence the fluxes of momentum by synoptic waves in the upper troposphere[19,40,41]. Theory dictates that the phase speed[42] and direction of propagation[41] of synoptic waves near the tropopause level are determined in part by the strength of the circulation there. (The phase speed is also determined by the length scale of the waves[43], although it remains to be demonstrated how ozone depletion can change the length scale.) The phase speed and direction of propagation of the synoptic waves are important, as they determine where the waves will break and thus decelerate the prevailing tropospheric eastward flow. Such wave-driven decelerations of the tropospheric flow drive changes in the north–south temperature gradient that extend to Earth's surface (for example through the aforementioned downward control), and thus can influence the near-surface wave fluxes of heat[13,44].

Despite continuing uncertainty in the physical mechanisms that drive the linkages between the ozone hole and the SAM, it is nevertheless clear that the linkages have important implications for surface climate variability in the Southern Hemisphere, as discussed in the following two sections.

Impacts on month-to-month timescales

The implications of the ozone hole for surface climate change will be discussed in two parts. In this section, we will review the summertime climate impacts of the SAM on month-to-month timescales. The signature of the SAM in the month-to-month variability can be assessed with a high degree of confidence in a relatively short data record, as the characteristic timescale of the SAM is only ~10 days. It also provides a framework for interpreting the effects of long-term changes in the SAM, assuming that the influence of the SAM on surface climate is not strongly timescale-dependent. In the subsequent section, we will discuss the implications of the trend in the SAM for long-term Southern Hemisphere climate change.

In the following, bear in mind that the high- and low-index polarities of the SAM are not distinct peaks in a bimodal frequency distribution but represent the wings of an approximately normally distributed frequency distribution[11]. The results shown in Figs 1–3 suggest that the ozone hole has shifted the frequency distribution of the SAM towards its high-index polarity, that is, that the ozone hole has led to an increased incidence of the high-index polarity of the SAM. For this reason, we will discuss the changes in climate associated with the high-index polarity of the SAM.

The summertime climate impacts of the Southern Hemisphere annular mode are wide and varied. Over high latitudes (~55–70° S), the high-index polarity of the SAM is characterized by nearly zonally symmetric eastward anomalies in the surface flow (acceleration of the prevailing eastward wind, Fig. 4a, b; anomalies are defined as departures from the long-term mean). Here, the high-index polarity is linked to lower than normal summertime temperatures over much of east Antarctica and higher than normal summertime temperatures over Patagonia and the northern reaches of the Antarctic Peninsula (Fig. 4a)[5,17,45,46]. The cooling over east Antarctica is consistent with anomalous rising motion and thus a suppression of the katabatic flow over the polar cap[6,46]; the warming over the Peninsula and Patagonia is consistent with increased warm temperature advection from the Southern Ocean due to the stronger eastward surface flow (Fig. 4a)[5,6,45,46]. Detailed analyses of station data indicate that the SAM has a much larger effect on surface temperatures over the eastern side of the Peninsula than the western side because of the orographic effects of the Antarctic Andes[45].

At middle latitudes (~35–50° S), the high-index polarity of the SAM is characterized by westward anomalies in the surface flow (deceleration of the prevailing eastward wind; Fig. 4b). Here, the anomalous flow leads to summertime increases in orographically induced precipitation on the eastern side of the Southern Alps of New Zealand (highlighted in Fig. 4d)[47–49] and of the Great Dividing Range of southeastern Australia (Fig. 4e)[50,51]. Similarly, it leads to a decrease in precipitation on the western slopes of the Southern Alps of New Zealand (Fig. 4d)[47–49] and the western half of Tasmania (Fig. 4e)[50], to higher than normal summertime temperatures throughout much of New Zealand (Fig. 4c)[47], and to lower than normal summertime temperatures over central and eastern subtropical Australia[50].

The high-index polarity of the SAM is also linked to pronounced summertime changes in the Southern Ocean (summarized in the schematic in Fig. 5). The anomalous eastward atmospheric flow centred near 60° S leads to increased equatorward Ekman transport over much of the Southern Ocean, and thus increased upwelling in the Southern Ocean poleward of 60° S and downwelling at middle latitudes[22,52–54]. Such changes are difficult to measure directly, but numerical experiments predict that on timescales shorter than a season, the changes in Ekman flow will tighten the north–south density gradients across the Southern Ocean, and shift the Antarctic Circumpolar Current and the upper limb of the Southern Ocean meridional overturning circulation poleward[27,53,55,56]. On timescales longer than a season, the Ekman-induced changes are predicted to be mostly compensated by the diffusion of density and heat by ocean eddies with length scales of ~10–100 km (refs 57–64). Recent work[65] argues that coarse-resolution models can approximately parameterize the eddy response so long as the applied coefficient of isopycnal thickness diffusion has an appropriate variable definition. Thus the ocean circulation response to the SAM consists of two components: a short-timescale component dominated by changes in the Ekman layer, and a long-timescale component in which diffusion by ocean eddies plays a key role.

At the ocean surface, the high-index polarity of the SAM is linked in observations and model experiments to lower than normal summertime sea-surface temperatures around most of Antarctica and higher than normal sea-surface temperatures in middle latitudes (Fig. 4b, 5)[56,66,67]. The changes in summertime sea-surface temperatures associated with the SAM are driven not only by changes in the ocean Ekman circulation, but also by the anomalous fluxes of sensible and latent heat at the atmosphere–ocean interface (Fig. 5)[56,66,67]. For example, the lower than normal sea-surface temperatures to the southeast of New Zealand (Fig. 4b) are consistent with enhanced ocean heat loss caused by the overlying wind anomalies. Changes

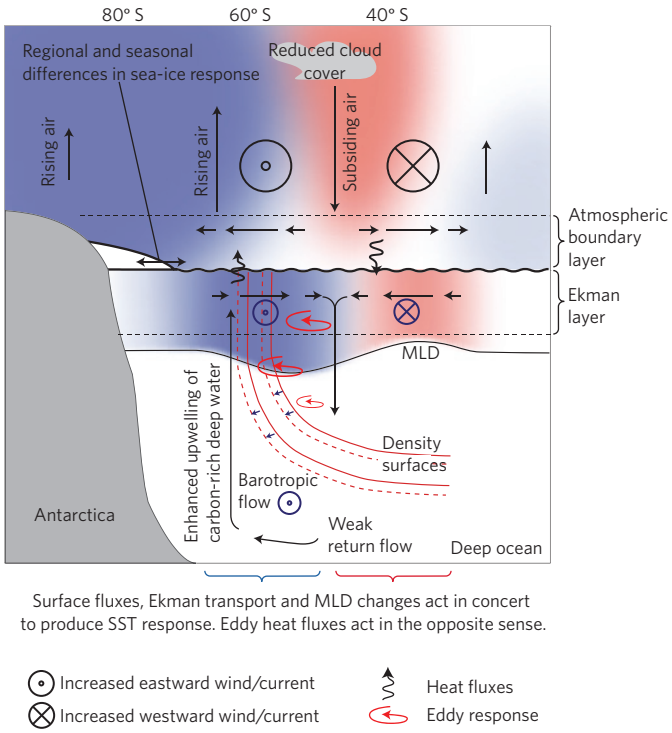

Surface fluxes, Ekman transport and MLD changes act in concert to produce SST response. Eddy heat fluxes act in the opposite sense.

Figure 5 | Schematic response of the ocean to the high-index polarity of the southern annular mode. Solid arrows indicate meridional and vertical motion in the atmosphere and ocean. Warm colours correspond to increases in temperature or heat content, and cooler colours to decreases. MLD refers to the ocean mixed-layer depth. All other responses are labelled on the figure or in the legend. All results indicate the climate response to the SAM on timescales less than a season with the exception of the oceanic eddy field, which indicates the response on timescales of 2–3 years (refs 108, 109). See text for details.

in cloudiness and the diffusion of heat by ocean eddies are also likely to influence the pattern of sea surface temperatures in Fig. 4b, but these effects have not yet been quantified.

Implications for long-term changes

The trend in the SAM from the pre-ozone-hole to ozone-hole eras (for example from the 1970s to the 2000s) is largest during the summer months, during which time its amplitude is roughly 0.5 standard deviations of its month-to-month variability per decade[15]. As noted earlier, the trend in the SAM is statistically distinct from estimates of natural variability, although its amplitude may change slightly depending on the precise start and end dates of the analysis (cf. Figure 7 of ref. 15). The trend in the SAM during winter months is not significant[15] and thus the SAM has not contributed in a significant manner to long-term changes in surface climate during the cold season.

The implications of the trend in the SAM for long-term changes in summertime surface climate can be inferred from knowledge of: (1) the signature of the SAM in the month-to-month variability (as reviewed in the previous section) and (2) the amplitude of the trend in the SAM. For example, if a change of 1 standard deviation in the SAM is associated with a 2 K change in local temperature in the month-to-month variability, then a long-term change in the SAM of 0.5 standard deviation (std) per decade is expected to drive a long-term change in local temperature of (2 K/1 std) × (0.5 std/decade) = 1 K per decade. Note that the extrapolation only holds if the signature of the SAM is stationary across monthly and decadal timescales.

The most robust (albeit spatially sparse) measurements available during both the pre-ozone-hole to ozone-hole eras include the ozonesonde, radiosonde and surface temperature data used in Fig. 1a and b, and Fig. 4a. The historical perspective provided by all three measurements types is key: the long-term ozonesonde records allow us to assess the scale of the ozone losses over Antarctica relative to the pre-ozone-hole era; the long-term radiosonde records allow us to link the Antarctic ozone losses to changes in the atmospheric circulation and the SAM; and the long-term surface temperature measurements allow us to make inferences about the influence of ozone depletion on temperature trends over Antarctica.

For example, the Antarctic Peninsula region warmed markedly during austral summer from the 1970s to the early 2000s[45,68–71]. The breakup of the Larsen-B ice shelf in 2002 was probably due at least in part to the remarkable warming in the Peninsula region[45]. In contrast, the high plateau and coastal regions of east Antarctica cooled during summertime over the same period[5,68]. During summer, roughly half of the warming of the Peninsula and almost all of the cooling over east Antarctica observed through the early 2000s is consistent with the observed trend towards the high index polarity of the SAM[5,17,45]. Because the trend in the SAM is confined to the summer months, the SAM is not linked to Antarctic temperature trends during other times of year (such as the wintertime warming over the Peninsula[68]). Nor is it clearly linked to temperature trends over West Antarctica[72], where changes in tropical sea-surface temperatures appear to play a role in long-term atmospheric temperature trends[73,74].

The SAM is also implicated in a range of climate trends over the Southern Ocean. The summertime trend in the SAM may have contributed to the observed warming and freshening of the subsurface Southern Ocean to depths up to ~1 km (refs 27,58,75–79), to changes in the South Pacific ocean at subtropical latitudes[80], and to a poleward shift of the frontal zones that delineate the Antarctic Circumpolar Current[61,81]. The trend in the SAM has been linked to potentially pronounced outgassing of ocean carbon dioxide[82–85], although observations are sparse[86] and the role of ocean eddies on the SAM-induced changes remains poorly understood[63,87]. The trend in the SAM has even been linked to changes in Earth's radiative balance: a recent model study suggests that the high-index polarity of the SAM generates more sea spray and thus cloud condensation nuclei for the formation of reflective low clouds over the high-latitude Southern Ocean[88], but these results have not been tested in observations.

On interannual timescales, the high-index polarity of the SAM is associated with summertime decreases in sea-ice near the Antarctic Peninsula, increases in sea ice near the Ross Sea, and weak increases in sea ice around much of Antarctica[89] (G. R. Simpkins, L. M. Ciasto, M. H. England & D. W. J. Thompson, manuscript in preparation). However, the trend in the SAM is not clearly linked to long-term changes in Southern Hemisphere sea ice in observations[90] (G. R. Simpkins, L. M. Ciasto, M. H. England, & D. W. J. Thompson, manuscript in preparation) and corroborating numerical evidence is sparse. Several experiments have considered the simulated sea-ice response to the SAM[91–93], but only one (ref. 93) attempts to isolate the role of the SAM in sea-ice trends (and that particular model suggests the SAM is not tied to Antarctic sea-ice trends); the others are run with prescribed sea ice (ref. 91) or driven by a range of forcings in addition to ozone depletion (ref. 92).

The trend in the SAM has been linked to the observed summertime increases in precipitation over southeastern Australia and eastern Tasmania over the period 1979–2005 (ref. 50). Stratospheric ozone depletion has also been linked to summertime changes in the subtropical circulation[24,25,28,32,33] and precipitation[28,32,33,94] in climate models. But observations suggest that the SAM cannot explain the

observed summertime increases in subtropical rainfall over northern Australia[50].

Confidence in the past and future outlook

Long-term changes in Southern Hemisphere climate are driven by a variety of factors, including increasing atmospheric greenhouse gases and changes in tropical sea-surface temperature. The evidence reviewed here suggests that they are also driven by Antarctic ozone depletion and recovery.

Our confidence in the linkages between the development of the Antarctic ozone hole and Southern Hemisphere surface climate changes stems from a variety of factors, including: (1) robust coupling between stratospheric variability and the annular modes on a range of timescales[6,7,9], not just in association with the ozone hole; (2) the reproducibility of the observed linkages between the ozone hole and the SAM in a hierarchy of models forced with either increases in ozone-depleting substances or depletion of polar stratospheric ozone[15,21–26,28–33]; and (3) the theoretical expectation that the climate response to external forcing will project onto internal modes of the climate system such as the SAM[95,96].

Our confidence in the linkages between the ozone hole and the SAM is limited by three primary caveats. First, we lack a quantitative and prognostic theory for dynamical coupling between the stratospheric and tropospheric circulations. Second, climate models have known deficiencies in simulating the mean climate over the high latitudes of the Southern Hemisphere[24]. And third, the existing model evidence is based on relatively few clean experiments, that is, experiments forced solely by changes in stratospheric ozone or ozone-depleting substances. The limited number of experiments is potentially problematic given the spread in climate model formulation and the large internal variability in the extratropical circulation.

As for the rest of the twenty-first century, climate change experiments reveal a robust SAM response to both future increases in greenhouse gases[25,27,28,31,32,97,99–104] and future recovery of the ozone hole[25–28,31,32,98,104]. As highlighted in Fig. 3 (using model output from ref. 28), ozone recovery is predicted to lead to a negative trend in the SAM that is limited to the summer months (Fig. 3a), whereas greenhouse gases are predicted to lead to a positive trend in the SAM that extends across both summer and winter (Fig. 3b). During summer over the next ~50 years, the effects of ozone recovery on the SAM are expected to be roughly equal but opposite to those due to increasing greenhouse gases. But during other seasons, increasing greenhouse gases are expected to drive a trend in the SAM towards its high index polarity that is unopposed by ozone recovery[24–28,31,32,98,104,105]. The SAM is expected to have a marked effect on future Southern Hemisphere climate change.

Methods

The composites in Fig. 1a, b and Fig. 2a are based on the mean differences between (i) years of large ozone depletion (1995–2009 with the exception of the 12-month period following the sudden warming of September 2002) and (ii) the pre-ozone-hole period of 1966–79 (for the radiosonde data in Fig. 1a) and 1979–85 (for the reanalysis data in Fig. 2a). The decreases in Z in Fig. 1b–d are indicative of eastward anomalies in the circumpolar flow of the polar vortex and thus the high index polarity of the SAM, and vice versa. For Fig. 1b, polar-mean Z is found by averaging over six radiosonde stations: Halley, 76° S, 27° W; Novolazaravskaja, 71° S, 12° E; Syowa, 69° S, 40° E; Mirnyj, 67° S, 93° E; Casey, 66° S, 111° E; and McMurdo, 78° S, 167° E. For Fig. 1c and d, polar-mean Z is found by averaging over 65° S to 90° S.

The grey shading in Fig. 3 denotes ± one standard deviation of the three ensemble members about the 50-year low-pass ensemble mean, calculated as a function of calendar year. For example, if $X(i,t)$ denotes the data for ensemble member i at year t, then the grey shading for year 1999 shows ± one standard deviation of the three ensemble members at t = 1999 about the 50-year low-pass ensemble mean at t = 1999.

The regressions in Fig. 4 are based on the 1979–2008 period for New Zealand/Australian temperatures, New Zealand/Australian precipitation, and sea surface temperatures; and on the 1979–2010 period for reanalysis winds and Antarctic surface temperatures. Regressions are based on standardized monthly mean values of the SAM index, which is defined here as the leading principal component time series of 850-hPa geopotential height anomalies from 20° S to 90° S. Figure 4a is adapted from ref. 5 and based on temperature data described in ref. 106; Fig. 4b is adapted from ref. 67; the data in Fig. 4c and d are courtesy of NIWA; the data in Fig. 4e are described in ref. 107, and are courtesy of CSIRO Australia.

References

1. World Meteorological Organization *Scientific Assessment of Ozone Depletion: 2010* Global Ozone Research and Monitoring Project Report No. 52 (WMO, 2011).
2. Solomon, S. Stratospheric ozone depletion: A review of concepts and history. *Rev. Geophys.* **37,** 275–316 (1999).
3. Randel, W. J. & Wu, F. Cooling of the Arctic and Antarctic polar stratosphere due to ozone depletion. *J. Clim.* **12,** 1467–1479 (1999).
4. Waugh, D. W., Randel, W. J. & Pawson, S. Persistence of the lower stratospheric polar vortices. *J. Geophys. Res.* **104,** 27191–27202 (1999).
5. Thompson, D. W. J. & Solomon, S. Interpretation of recent Southern Hemisphere climate change. *Science* **296,** 895–899 (2002).
6. Thompson, D. W. J. & Wallace, J. M. Annular modes in the extratropical circulation. Part I: Month-to-month variability. *J. Clim.* **13,** 1000–1016 (2000).
7. Baldwin, M. P. & Dunkerton, T. J. Stratospheric harbingers of anomalous weather regimes. *Science* **244,** 581–584 (2001).
8. Graversen, R. G. & Christiansen, B. Downward propagation from the stratosphere to the troposphere: A comparison of the two hemispheres. *J. Geophys. Res.* **108,** 4780 (2003).
9. Thompson, D. W. J., Baldwin, M. P. & Solomon, S. Stratosphere–troposphere coupling in the Southern Hemisphere. *J. Atmos. Sci.* **62,** 708–715 (2005).
10. Karoly, D. J. The role of transient eddies in low-frequency zonal variations of the Southern Hemisphere circulation. *Tellus* **42A,** 41–50 (1990).
11. Hartmann, D. L. & Lo, F. Wave-driven zonal flow vacillation in the Southern Hemisphere. *J. Atmos. Sci.* **55,** 1303–1315 (1998).
12. Limpasuvan, V. & Hartmann, D. L. Wave-maintained annular modes of climate variability. *J. Clim.* **13,** 4414–4429 (2000).
13. Lorenz, D. J. & Hartmann, D. L. Eddy-zonal flow feedback in the Southern Hemisphere. *J. Atmos. Sci.* **58,** 3312–3327 (2001).
14. Barnes, E. A. & Hartmann, D. L. Dynamical feedbacks of the Southern Annular Mode in winter and summer. *J. Atmos. Sci.* **67,** 2320–2330 (2010).
15. Fogt, R. L. *et al.* Historical SAM variability. Part II: Twentieth-century variability and trends from reconstructions, observations, and the IPCC AR4 models. *J. Clim.* **22,** 5346–5365 (2009).
16. Marshall, G. J. Trends in the Southern Annular Mode from observations and reanalyses. *J. Clim.* **16,** 4134–4143 (2003).
17. Marshall, G. J. Half-century seasonal relationships between the Southern Annular Mode and Antarctic temperatures. *Int. J. Climatol.* **27,** 373–383 (2007).
18. Polvani, L. M. & Kushner, P. J. Tropospheric response to stratospheric perturbations in a relatively simple general circulation model. *Geophys. Res. Lett.* **29,** (2002).
19. Kushner, P. J. & Polvani, L. M. Stratosphere-troposphere coupling in a relatively simple AGCM: The role of eddies. *J. Clim.* **17,** 629–639 (2004).
20. Butler, A. H., Thompson D. W. J. & Heikes, R. The steady-state atmospheric circulation response to climate change-like thermal forcings in a simple general circulation model. *J. Clim.* **23,** 3474–3496 (2010).
21. Miller, R. L., Schmidt, G. A. & Shindell, D. T. Forced annular variations in the 20th century Intergovernmental Panel on Climate Change Fourth Assessment Report models. *J. Geophys. Res.* **111,** D18101 (2006).
22. Cai, W. & Cowan, T. Trends in Southern Hemisphere circulation in IPCC AR4 models over 1950–99: Ozone depletion versus greenhouse forcing. *J. Clim.* **20,** 681–693 (2007).
23. Karpechko, A., Gillett, N. P., Marshall, G. J. & Scaife, A. A. Stratospheric influence on circulation changes in the Southern Hemisphere troposphere in coupled climate models. *Geophys. Res. Lett.* **35,** L20806 (2008).
24. Son, S-W. *et al.* Impact of stratospheric ozone on Southern Hemisphere circulation change: A multimodel assessment. *J. Geophys. Res.* **115,** D00M07 (2010).
25. Son, S-W., Tandon, N. F., Polvani, L. M. & Waugh, D. W. Ozone hole and Southern Hemisphere climate change. *Geophys. Res. Lett.* **36,** L15705 (2009).
26. Son, S-W. *et al.* The impact of stratospheric ozone recovery on the Southern Hemisphere westerly jet. *Science* **320,** 1486–1489 (2008).
27. Sigmond, M., Reader, M. C., Fyfe, J. C. & Gillett, N. P. Drivers of past and future Southern Ocean change: stratospheric ozone verses greenhouse gas impacts. *Geophys. Res. Lett.* **38,** L12601 (2011).
28. McLandress, C. *et al.* Separating the dynamical effects of climate change and ozone depletion: Part 2. Southern Hemisphere troposphere. *J. Clim.* **24,** 1850–1868 (2011).

29. Sexton, D. M. H. The effect of stratospheric ozone depletion on the phase of the Antarctic Oscillation. *Geophys. Res. Lett.* **28,** 3697–3700 (2001).
30. Gillett, N. P. & Thompson, D. W. J. Simulation of recent Southern Hemisphere climate change. *Science* **302,** 273–275 (2003).
31. Shindell, D. & Schmidt, G. A. Southern Hemisphere climate response to ozone changes and greenhouse gas increases. *Geophys. Res. Lett.* **31**, L18209 (2004).
32. Arblaster, J. M. & Meehl, G. A. Contributions of external forcings to Southern Annular Mode trends. *J. Clim.* **19,** 2896–2905 (2006).
33. Polvani, L. M., Waugh, D. W., Correa, G. J. P. & Son, S-W. Stratospheric ozone depletion: The main driver of 20th century atmospheric circulation changes in the Southern Hemisphere. *J. Clim.* **24,** 795–812 (2011).
34. Sigmond, M., Fyfe, J. C. & Scinocca, J. F. Does the ocean impact the atmospheric response to stratospheric ozone depletion? *Geophys. Res. Lett.* **37,** L12706 (2010).
35. Held, I. M. The macroturbulence of the troposphere. *Tellus* **51A-B,** 59–70 (1999).
36. Grise, K. M., Thompson, D. W. J. & Forster, P. M. On the role of radiative processes in stratosphere–troposphere coupling. *J. Clim.* **22,** 4154–4161 (2009).
37. Haynes, P. H., McIntyre, M. E., Shepherd, T. G., Marks, C. J. & Shine, K. P. On the "downward control" of extratropical diabatic circulations by eddy-induced mean zonal forces. *J. Atmos. Sci.* **48,** 651–680 (1991).
38. Song, Y. & Robinson, W. A. Dynamical mechanisms for stratospheric influences on the troposphere. *J. Atmos. Sci.* **61,** 1711–1725 (2004).
39. Thompson, D. W. J., Furtado, J. C. & Shepherd, T. G. On the tropospheric response to anomalous stratospheric wave drag and radiative heating. *J. Atmos. Sci.* **63,** 2616–2629 (2006).
40. Wittman, M. A. H., Charlton, A. J. & Polvani, L. M. The effect of lower stratospheric shear on baroclinic instability. *J. Atmos. Sci.* **64,** 479–496 (2007).
41. Simpson, I. R., Blackburn, M. & Haigh, J. D. The role of eddies in driving the tropospheric response to stratospheric heating perturbations. *J. Atmos. Sci.* **66,** 1347–1365 (2009).
42. Chen, G. & Held, I. Phase speed spectra and the recent poleward shift of Southern Hemisphere surface westerlies. *Geophys. Res. Lett.* **34,** L21805 (2007).
43. Kidston, J., Vallis, G. K., Dean, S. M. & Renwick, J. A. Can the increase in the eddy length scale under global warming cause the poleward shift of the jet streams? *J. Clim.* **24,** 3764–3780 (2011).
44. Robinson, W. A. A baroclinic mechanism for the eddy feedback on the zonal index. *J. Atmos. Sci.* **57,** 415–422 (2000).
45. Marshall, G. J., Orr, A., van Lipzig, N. P. M. & King, J. C. The impact of a changing Southern Hemisphere Annular Mode on Antarctic peninsula summer temperatures. *J. Clim.* **19,** 5388–5404 (2006).
46. Van den Broeke, M. R. & van Lipzig, N. P. M. Changes in Antarctic temperature, wind and precipitation in response to the Antarctic Oscillation. *Ann. Glaciol.* **39,** 199–126 (2004).
47. Renwick, J. A. & Thompson, D. W. J. The Southern Annular Mode and New Zealand climate. *Water Atmos.* **14,** 24–25 (2006).
48. Griffiths, G. M. Changes in New Zealand daily rainfall extremes 1930 – 2004. *Weather and Climate* **26,** 3–46 (2006).
49. Ummenhofer, C. C., Sen Gupta, A. & England, M. H. Causes of late twentieth-century trends in New Zealand precipitation. *J. Climate*, **22,** 3–19 (2009).
50. Hendon, H. H., Thompson, D. W. J. & Wheeler, M. C. Australian rainfall and surface temperature variations associated with the Southern Hemisphere Annular Mode. *J. Clim.* **20,** 2452–2467 (2007).
51. Meneghini, B., Simmonds, I. & Smith, I. N. Association between Australian rainfall and the Southern Annular Mode. *Int. J. Climatol.* **27,** 109–121 (2007).
52. Oke, P. R. & England, M. H. Oceanic response to changes in the latitude of the Southern Hemisphere subpolar westerly winds. *J. Clim.* **17,** 1040–1054 (2004).
53. Fyfe, J. C. & Saenko, O. A. Simulated changes in the extratropical Southern Hemisphere winds and currents. *Geophys. Res. Lett.* **33,** L06701 (2006).
54. Fyfe, J. C., Saenko, O. A., Zickfeld, K., Eby, M. & Weaver, A. J. The role of poleward-intensifying winds on Southern Ocean warming. *J. Clim.* **20,** 5391–5400 (2007).
55. Hall, A. & Visbeck, M. Synchronous variability in the Southern Hemisphere atmosphere, sea ice, and ocean resulting from the Annular Mode. *J. Clim.* **15,** 3043–3057 (2002).
56. Sen Gupta, A. & England, M. H. Coupled ocean-atmosphere-ice response to variations in the Southern Annular Mode. *J. Clim.* **19,** 4457–4486 (2006).
57. Hallberg, R. & Gnanadesikan, A. The role of eddies in determining the structure and response of the wind-driven Southern Hemisphere overturning: Results from the Modeling Eddies in the Southern Ocean (MESO) project. *J. Phys. Ocean.* **36,** 2232–2252 (2006).
58. Böning, C. W., Dispert, A., Visbeck, M., Rintoul, S. R. & Schwarzkopf, F. U. The response of the Antarctic Circumpolar Current to recent climate change. *Nature Geosci.* **1,** 864–869 (2008).
59. Screen, J. A., Gillett, N. P., Stevens, D. P., Marshall, G. J. & Roscoe, H. K. The role of eddies in the Southern Ocean temperature response to the Southern Annular Mode. *J. Clim.* **22,** 806–818 (2009).
60. Hogg, A., Meredith, M., Blundell, J. & Wilson, C. Eddy heat flux in the Southern Ocean: Response to variable wind forcing. *J. Clim.* **21,** 608–620 (2008).
61. Salleé, J. B., Speer, K. & Morrow, R. Response of the Antarctic Circumpolar Current to atmospheric variability. *J. Clim.* **21,** 3020–3039 (2008).
62. Spence, P., Fyfe, J. C., Montenegro, A. & Weaver, A. J. Southern Ocean response to strengthening winds in an eddy-permitting global climate model. *J. Clim.* **23,** 5332–5343 (2010).
63. Farneti, R., Delworth, T. L., Rosati, A. J., Griffies, S. M. & Zeng, F. The role of mesoscale eddies in the rectification of the Southern Ocean response to climate change. *J. Phys. Oceanogr.* **40,** 1539–1557 (2010).
64. Farneti, R. & Delworth, T. L. The role of mesoscale eddies in the remote oceanic response to altered Southern Hemisphere winds. *J. Phys. Oceanogr.* **40,** 2348–2354 (2010).
65. Gent, P. R. & Danabasoglu, G. Response to increasing Southern Hemisphere winds in CCSM4. *J. Clim.* **24,** 4992–4998 (2011).
66. Verdy, A., Marshall, J. & Czaja, A. Sea surface temperature variability along the path of the Antarctic Circumpolar Current. *J. Phys. Oceanogr.* **36,** 1317–1331 (2006).
67. Ciasto, L. M. & Thompson, D. W. J. Observations of large-scale ocean–atmosphere interaction in the Southern Hemisphere. *J. Clim.* **21,** 1244–1259 (2008).
68. Turner, J. *et al.* Antarctic climate change during the last 50 years. *Int. J. Climatol.* **25,** 279–294 (2005).
69. Chapman, W. L. & Walsh, J. E. A synthesis of Antarctic temperatures. *J. Climate*, **20,** 4096–4117 (2007).
70. Monaghan, A. J., Bromwich, D. H., Chapman, W. & Comiso, J. C. Recent variability and trends of Antarctic near-surface temperature. *J. Geophys. Res.* **113,** D04105 (2008).
71. Zazulie, N., Rusticucci, M. & Solomon, S. Changes in climate at high southern latitudes: A unique daily record at Orcadas spanning 1903–2008 *J. Clim.* **23,** 189–196 (2010).
72. Steig, E. J. *et al.* Warming of the Antarctic ice sheet surface since the 1957 International Geophysical Year. *Nature* **457,** 459–462 (2009).
73. Schneider, D. P., Deser, C. & Okumura, Y. An assessment and interpretation of the observed warming of West Antarctica in the austral spring. *Clim. Dyn.* http://dx.doi.org/10.1007/s00382-010-0985-x (in the press).
74. Ding, Q., Steig, E. J., Battisti, D. S. & Küttel, M. Winter warming in West Antarctica caused by central tropical Pacific warming. *Nature Geosci.* **4,** 398–403 (2011).
75. Gille, S. T. Warming of the Southern Ocean since the 1950s. *Science* **295,** 1275–1277 (2002).
76. Gille, S. T. Decadal-scale temperature trends in the Southern Hemisphere ocean. *J. Clim.* **21,** 4749–4765 (2008).
77. Fyfe, J. C. Southern Ocean warming due to human influence. *Geophys. Res. Lett.* **33,** L19701 (2006).
78. Aoki, S., Yoritaka, M. & Masuyama, A. Multidecadal warming of subsurface temperature in the Indian sector of the Southern Ocean. *J. Geophys Res.* **108,** 8081 (2003).
79. Sprintall, J. Long-term trends and interannual variability of temperature in Drake Passage. *Prog. Ocean.* **77,** 316–330 (2008).
80. Roemmich, D. *et al.* Decadal spinup of the South Pacific subtropical gyre. *J. Phys. Ocean.* **37,** 162–173 (2007).
81. Sokolov, S. & Rintoul, S. R. The circumpolar structure and distribution of the Antarctic Circumpolar Current fronts. Part 2: Variability and relationship to sea surface height. *J. Geophys. Res.* **114,** C11019 (2009).
82. Lovenduski, N. S. & Gruber, N. Impact of the Southern Annular Mode on Southern Ocean circulation and biology. *Geophys. Res. Lett.* **32,** L11603 (2005).
83. Le Quéré, C. *et al.* Saturation of the Southern Ocean CO_2 sink due to recent climate change. *Science* **316,** 1735–1738 (2007).
84. Lenton, A. *et al.* Stratospheric ozone depletion reduces ocean carbon uptake and enhances ocean acidification. *Geophys. Res. Lett.* **36,** L12606 (2009).
85. Butler, A. H., Thompson, D. W. J. & Gurney, K. R. Observed relationships between the Southern Annular Mode and atmospheric carbon dioxide. *Global Biogeochem. Cycles* **21,** GB4014 (2007).
86. Metzl, N., Brunet, C., Jabaud-Jan, A., Poisson, A. & Schauer, B. Summer and winter air–sea CO_2 fluxes in the Southern Ocean. *Deep-Sea Res. I* **53,** 1548–1563 (2006).
87. Ito, T., Woloszyn, M. & Mazloff, M. Anthropogenic carbon dioxide transport in the Southern Ocean driven by Ekman flow. *Nature* **463,** 80–83 (2010).
88. Korhonen, H. *et al.* Aerosol climate feedback due to decadal increases in Southern Hemisphere wind speeds. *Geophys. Res. Lett.* **37,** L02805 (2010).
89. Lefebvre, W., Goosse, H., Timmermann, R. & Fichefet, T. Influence of the Southern Annular Mode on the sea ice–ocean system. *J. Geophys. Res.* **109,** C09005 (2004).

90. Renwick, J. A. Southern Hemisphere circulation and relations with sea ice and sea surface temperature. *J. Clim.* **15,** 3058–3068 (2002).
91. Turner, J. *et al.* Non-annular atmospheric circulation change induced by stratospheric ozone depletion and its role in the recent increase of Antarctic sea ice extent. *Geophys. Res. Lett.* **36**, L08502 (2009).
92. Goosse, H., Lefebvre, W., de Montety, A., Crespin, E. & Orsi, A. H. Consistent past half-century trends in the atmosphere, the sea ice & the ocean at high southern latitudes. *Clim. Dyn.* **33,** 999–1016 (2009).
93. Sigmond, M. & Fyfe., J. C. Has the ozone hole contributed to increased Antarctic sea ice extent? *Geophys. Res. Lett.* **37,** L18502 (2010).
94. Kang, S. M., Polvani, L. M., Fyfe, J. C. & Sigmond, M. Impact of polar ozone depletion on subtropical precipitation. *Science* **332,** 951–954 (2011).
95. Gerber, E. P., Polvani, L. M. & Ancukiewicz, D. Annular mode time scales in the Intergovernmental Panel on Climate Change Fourth Assessment Report models. *Geophys. Res. Lett.* **35,** L22707 (2008).
96. Ring, M. J. & Plumb, R. A. The response of a simplified GCM to axisymmetric forcings: Applicability of the fluctuation–dissipation theorem. *J. Atmos. Sci.* **65,** 3880–3898 (2008).
97. Fyfe, J. C., Boer, G. J. & Flato, G. M. The Arctic and Antarctic oscillations and their projected changes under global warming. *Geophys. Res. Lett.* **26,** 1601–1604 (1999).
98. Perlwitz, J., Pawson, S., Fogt, R. L., Nielsen, J. E. & Neff, W. D. Impact of stratospheric ozone hole recovery on Antarctic climate. *Geophys. Res. Lett.* **35,** L08714 (2008).
99. Kushner, P., Held, I. M. & Delworth, T. L. Southern Hemisphere atmospheric circulation response to global warming. *J. Clim.* **14,** 2238–2249 (2001).
100. Cai, W., Whetton, P. & Karoly, D. The response of the Antarctic Oscillation to increasing and stabilized atmospheric CO_2. *J. Clim.* **16,** 1525–1538 (2003).
101. Brandefelt, J. & Kallen, E. The response of the Southern Hemisphere atmospheric circulation to an enhanced greenhouse gas forcing. *J. Clim.* **17,** 4425–4442 (2004).
102. Yin, J. H. A consistent poleward shift of the storm tracks in simulations of 21st century climate. *Geophys. Res. Lett.* **32,** L18701 (2005).
103. Lu, J., Chen, G. & Frierson, D. Response of the zonal mean atmospheric circulation to El Niño versus global warming. *J. Clim.* **21,** 5835–5851 (2008).
104. Arblaster, J. M., Meehl, G. A. & Karoly, D. J. Future climate change in the Southern Hemisphere: Competing effects of ozone and greenhouse gases. *Geophys. Res. Lett.* **38,** L02701 (2011).
105. Polvani, L. M., Previdi, M. & Deser, C. Large cancellation, due to ozone recovery, of future Southern Hemisphere atmospheric circulation trends. *Geophys. Res. Lett.* **38,** L04707 (2011).
106. Brohan, P., Kennedy, J. J., Harris, I., Tett, S. F. B. & Jones, P. D. Uncertainty estimates in regional and global observed temperature changes: A new dataset from 1850. *J. Geophys. Res.* **111,** D12106 (2006).
107. Jones, D. A., Wang, W. & Fawcett, R. High-quality spatial climate data-sets for Australia. *Aust. Meteorol. Oceanogr. J.* **58,** 233–248 (2009).
108. Meredith, M. P. & Hogg, A. M. Circumpolar response of Southern Ocean eddy activity to a change in the Southern Annular Mode. *Geophys. Res. Lett.* **33,** L16608 (2006).
109. Morrow, R., Ward, M. L., Hogg, A. M. & Pasquet, S. Eddy response to Southern Ocean climate modes. *J. Geophys. Res.* **115,** C10030 (2010).

Acknowledgements

We thank N. Gillett, L. Polvani and C. McLandress for providing the model output shown in Figs 1, 2 and 3 (as noted in the figure legends); A. Santoso for generating Fig. 3; L. Ciasto for generating the results shown in Fig. 4b; J. Renwick for providing the New Zealand temperature and precipitation data used in Fig. 4c, d; C. Ummenhofer for assistance with the data for Fig. 4e; and A. Sen Gupta for generating Fig. 5. Thanks also to J. Arblaster, J. Fyfe, N. Gillett, I. Held, H. Hendon, A. Hogg, C. Le Quéré, C. McLandress, L. Polvani, J. Renwick, S-W. Son and S. Rintoul for discussions and comments on the manuscript. D.W.J.T. is funded by the National Science Foundation Climate Dynamics program and appreciates sabbatical funding provided by the Climate Change Research Centre at UNSW, where much of the text was written. D.J.K. is supported by the Australian Research Council through the Discovery Projects funding scheme (Project FF0668679). M.H.E. is supported by the Australian Research Council through the Laureate Fellowships funding scheme (Project FL100100214). P.J.K. acknowledges support of the Canadian Foundation for Climate and Atmospheric Sciences and the Natural Sciences and Engineering Research Council of Canada.

Additional information

The authors declare no competing financial interests.